



Self-buckling-restrained steel plate shear wall made by two diagonally corrugated infill plates

M. Masoumi¹ · F. Emami¹ · P. Javadi¹

Received: 5 July 2021 / Accepted: 24 January 2022 / Published online: 19 March 2022
© The Author(s), under exclusive licence to Springer Nature Switzerland AG 2022

Abstract

In this paper, the seismic behavior of a novel steel plate shear wall (SPSW) has been presented. This SPSW consists of two diagonally corrugated infill plates (2DCIPs) which were tied to each other as an infill plate and a one-bay one-story moment-resisting frame as a boundary element. The direction of two diagonally corrugated infill plates (DCIP) is reversed. When one of the DCIPs is compressed, the other DCIP is tensioned providing the lateral support for the DCIP in compression. The behavior of the SPSW with 2DCIPs was compared to one Solid Infill Plate (SIP) and with one Corrugated Infill Plate (CIP) to show the advantages and disadvantages of the new SPSW. According to the results, the advantages of the new SPSW can be the shear strength increase (in infill plates with a thickness greater than 8 mm), energy dissipation increase, a suitable response modification factor, reduction of the force applied to the column from the infill plate, limitation of the buckling on the infill plate and the prevention of the resistance drop (in the CIP). In general, it can be said that the new SPSW, has almost all the advantages of SIP and CIP. Further, a set of parametric studies was performed to investigate the hysteretic behavior of the SPSW with 2DCIPs. These parameters included the infill plate thickness, the angle of the DCIP with the frame, the wave length of corrugation, the angle of the sub-plates of the DCIP and the adhesive thickness.

Keywords Steel plate shear wall · Self-buckling-restrained · Diagonally corrugated · Response modification factor · Hysteretic behavior · Energy dissipation

Introduction

The main function of the steel plate shear wall (SPSW) is to resist horizontal shear story and overturning moment resultant from the lateral loads. Steel frame and infill plate acting as boundary component and energy dissipation device respectively, constitute the elements of the SPSW system. The advantages of this system include high elastic stiffness, stable hysteretic behavior, high energy dissipation capacity and the suitable response modification factor.

A wide variety of researches has been done on the various parameters of the SPSW, among which can be mentioned to

the examination of the influence of the material and properties of the infill plates (Caccese et al., 1993; Edalati et al., 2015; Soltani et al., 2017; Zirakian & Zhang, 2016), the inclination angle of tension field action (Timler & Kulak, 1983), the infill plate thickness (Elgaaly et al., 1993), hole creation in the infill plates (Ali et al., 2018; Roberts & Sabouri-Ghomi, 1992), the specifications of connecting the beam to column (Driver et al., 1998; Elgaaly et al., 1993; Roberts & Sabouri-Ghomi, 1992), the infill plate-frame connection (Elgaaly, 1998), utilizing the reduced beam section in the SPSW (Qu & Bruneau, 2011) and Optimal seismic design of steel plate shear walls (Kaveh & Farhadmanesh, 2019).

Developing and using the low-yield point (LYP) infill plates as the SPSW successfully in Japan is based on the findings pertinent to the research carried out by Nakashima et al. (1994). Low yield point approximately half yield point of A36 steel along with higher ductility as well as higher ultimate strain (more than twice that of A36 steel) are important properties of LYP steel. Based on the foregoing, such

✉ F. Emami
f-emami@srbiau.ac.ir

M. Masoumi
mehdi1991masoumi@gmail.com

P. Javadi
Javadi@srbiau.ac.ir

¹ Department of Civil Engineering, Science and Research Branch, Islamic Azad University, Tehran, Iran

steel has been proven to be used effectively in Japan, acting as an energy dissipation element of the structure.

Earlier, the SPSW used in the United States and Japan had infill plates with horizontal and vertical stiffeners. Based on the studies and realistic experimental specimens, welding the stiffeners to the infill plate leads to increase the shear yield strength of the SPSW and act as a very ductile, desirable and efficient system (Astaneh-Asl, 2001). In further research on the SPSW, Hitaka and Matsui (2003), investigated an SPSW with Slits. The steel plate between two slots could behave as a flexural link, and endure large flexural deformations which were the contributions of the infill plate slot.

Research on the SPSW with CIP was conducted by Bremen and Bruneau (2005). Two samples of SIP with a thickness of 0.9 mm and diagonal CIP with a thickness of 0.7 were investigated. The results showed that the SIP is more ductile. The hysteretic curve of the CIP was asymmetric; so, the proposed 2-bay application with the opposite CIP direction was presented. In the next study by Emami et al., (2013), some experiments were conducted on the SPSW with CIP. In total, they compared three samples (SIP, vertical and horizontal trapezoidal CIP) to investigate and determine the hysteretic behavior of the trapezoidally corrugated SPSW. The laboratory results showed that although the ultimate strength of the SPSW with CIP has decreased, it shows better behavior in terms of energy dissipation and ductility. Afterwards, other studies were conducted on the SPSW with CIP (Dou et al., 2018, 2021; Emami & Mofid, 2014; Kalali et al., 2015; Shariati et al., 2019).

Wang et al. (2017) studied the seismic behavior of the Self-Buckling-Restrained (SBR) SPSW, which consists of

two incline-slotted infill plates (2ISIPs). They examined the SBR mechanism in the SPSW. Afterwards, another study was conducted on the SPSW with double corrugated infill plates with the same direction in the frame (Tong et al., 2020). In present study, a new SBR-SPSW which consists of two trapezoidal CIPs that the plates are placed diagonally in a 45-degree angle but in an opposite direction in one-bay one-story moment-resisting frame as Fig. 1 and two infill plates are connected to each other by an adhesive was introduced for high-rise structures. When one of the DCIP is under compression, the other DCIP is tensioned providing lateral support for the DCIP in compression. The benefits of the SBR-SPSW made by 2DCIPs compared to the SPSW with SIP and CIP include the following:

1. In various types of the SPSWs including the infill plates with the opening, the infill plates using LYP steel, infill plates with holes (Bhowmick et al., 2014), and infill plates with slits, smaller shear strength are observed compared to the SPSW with the SIP; but, the SPSW with 2DCIPs with an overall thickness greater than 8 mm have a higher shear strength compared to the SPSW with the SIP. In the SIP with a thickness of more than 8 mm, the shear strength is not proportional to the increase in thickness; hence, the use of low-thickness infill plates is always advisable; but in 2DCIPs, this deficit of SIP has been somewhat improved.
2. In 2DCIPs, the yielding occurred on the infill plates before the frame.

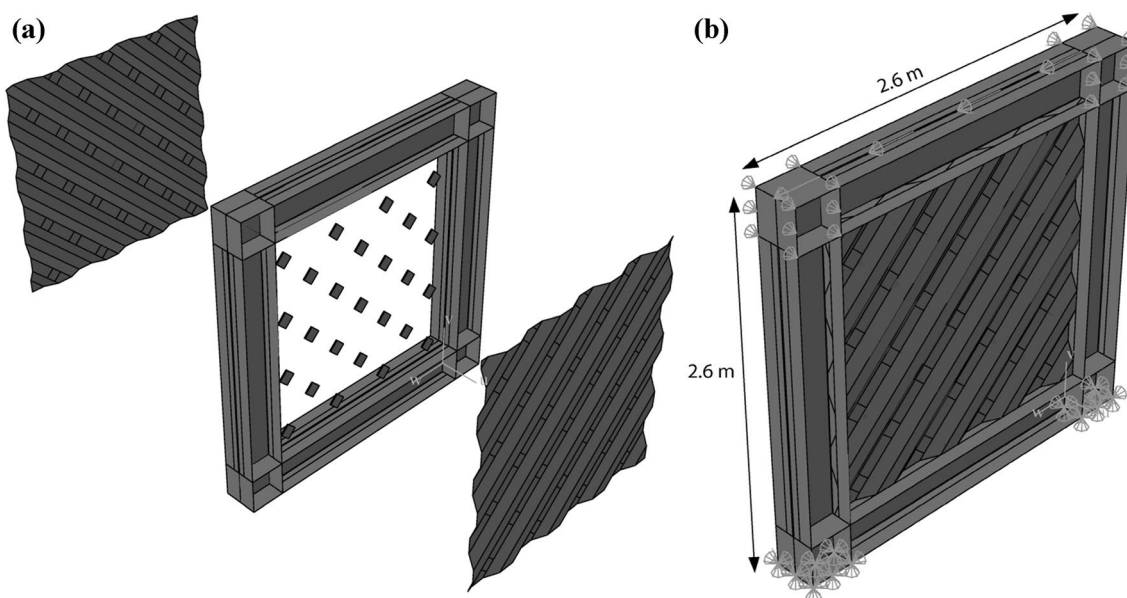


Fig. 1 Configuration details **a** Position of SBR-SPSW made by 2DCIPs; **b** the Boundary conditions

3. The SBR-SPSW made by 2DCIPs has a high energy dissipation capacity compared to the SPSW with SIP and CIP.
4. In the SPSW with CIP (the CIPs directioned horizontally or vertically), resistance drop is observed; but, in the SBR-SPSW made by 2DCIPs, resistance drop can be prevented.
5. The lateral support of the DCIPs for each other has led to a limitation of buckling in 2DCIPs
6. The use of two infill plates, which are under relative tension and compression, has led to a reduction in the force on the column from the 2DCIPs.
7. In the SBR-SPSW made by 2DCIPs, though in some thicknesses, compared to the SPSW with SIP, a slight decrease in the response modification factor was observed, but compared with the SPSW with CIP, there has been always a significant increase in the response modification factor.

$$\mu_s = \frac{\Delta_{max}}{\Delta_y} \tag{1}$$

$$\left. \begin{aligned} R &= \frac{V_e}{V_s} = R_\mu \times \Omega_o \\ R_\mu &= \frac{v_e}{v_y}, \Omega_o = \frac{v_y}{v_s} \end{aligned} \right\} \tag{2}$$

Figure 2 shows how to draw an idealized bilinear response curve based on the actual inelastic response curve and a sample of the displacement curve with an idealized bilinear response curve for SBR-SPSW-2DCIPs with a total thickness (t_t) of 8 mm. To draw the idealized bilinear response curve using the actual inelastic response curve, first, extend the slope of the elastic region (V_s/Δ_s) to V_y , and then connect it to the endpoint of actual inelastic response curve; it is noteworthy that V_y has been chosen in a way that the area under the idealized bilinear response curve is equal to the area under the actual inelastic response curve.

Calculation of the response modification factor and verification of the finite element model

Calculation of the response modification factor

Uang (1991) presented Eqs. 1, 2 for calculating the ductility factor and the response modification factor where μ_s is the ductility factor, R_μ is the ductility reduction factor, Ω_o is the overstrength factor, R is the response modification factor, V_e is the ultimate elastic base shear, V_s is the base shear at the first significant yield, V_y is the yield strength which is equal to the base shear at the structural collapse level, Δ_y is the drift at the corresponding yield strength, Δ_s is the drift at the first significant yield, and Δ_{max} is the maximum amount of the drift.

Design of the SPSW

The AISC (2010) describes that the Vertical Boundary Elements (VBEs) should have the moments of inertia (I_c) not less than Eq. 3, and the Horizontal Boundary Elements (HBEs) should have the moments of inertia (I_b) not less than Eq. 4, and also the Eq. 5 is presented for the width-to-height ratio. The geometric characteristics of the boundary elements and infill plate are presented in Table 1, meeting the design requirements.

$$I_c \geq 0.0031 \times t_w \frac{h_s^4}{L} \tag{3}$$

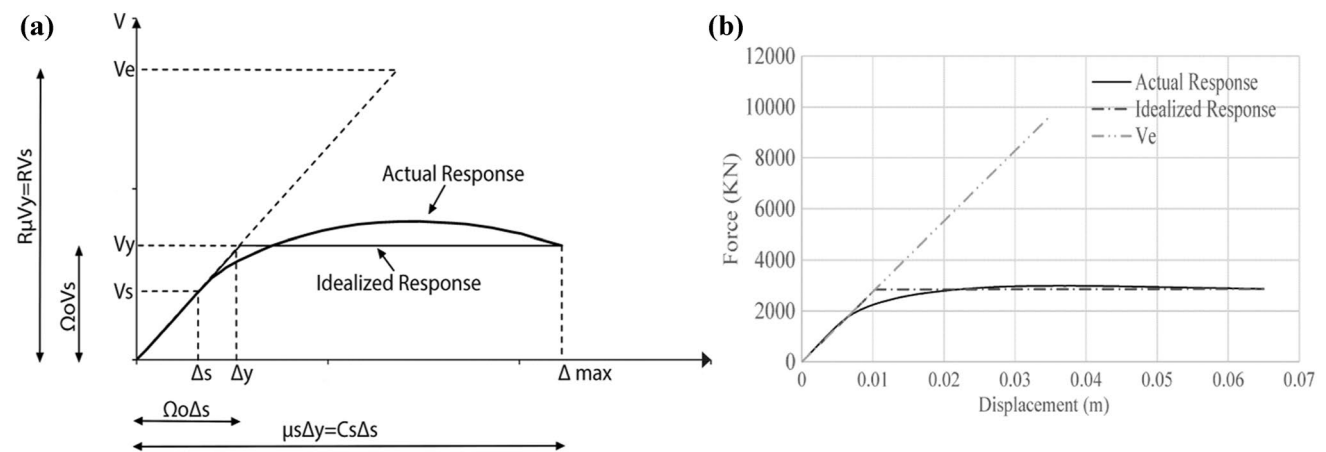


Fig. 2 Draw an idealized bilinear response curve a General structural response; b the sample

Table 1 Geometric characteristics of the boundary element and infill plates

	Infill plates				Boundary element				
	l (mm)	h (mm)	tw (mm) tt (mm)	Steel type	bf (mm)	hf (mm)	tf (mm)	tw(BE) (mm)	Steel type
DCIPs SIP CIP	2000	2000	2,3,4,8,10	A36	300	300	16	16	A572 grade50

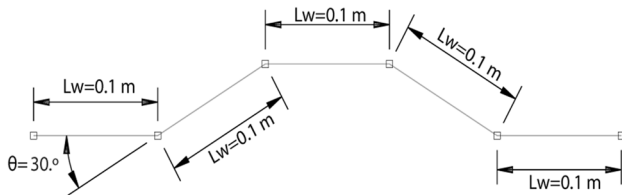


Fig. 3 Geometric properties of trapezoidally corrugated plate (m)

$$I_b \geq 0.0031 \times \Delta t_w \frac{L^4}{h_s} \tag{4}$$

$$0.8 \leq \frac{L}{h_s} \leq 2.5 \tag{5}$$

Where L is the distance between VBE centerlines, h_s is the distance between HBE centerlines, t_w is the thickness of the shear panel, and Δt_w is the difference in the shear panel thicknesses above and below.

The diagonal tension field inclination angle, as measured relative to the vertical, is dependent on the geometric specifications of the boundary elements (including beam and column). The inclination angle, α , can be calculated as Eq. 6:

$$\alpha = \arctg^4 \sqrt{\frac{1 + \frac{t_w \times L}{2A_c}}{1 + t_w \times h_s \times \left[\frac{1}{A_b} + \frac{h_s^3}{360 \times I_c \times L} \right]}} \tag{6}$$

Where A_b is the cross-sectional area of an HBE and A_c is the cross-sectional area of a VBE. Dimensions and geometric characteristics of trapezoidal CIP are seen in Fig. 3 (units are based on m and degree). In this figure L_w is the wavelength of corrugation and θ is the angle of the sub-plates of the CIP. It should be noted that the angle of the DCIP with the frame (α) shown in Fig. 4 is 45°.

Finite element model (FEM)

The seismic behavior of an SBR-SPSW made by 2DCIPs was investigated using the finite element analyses in one-bay one-story moment-resisting frame. In this study, the infill

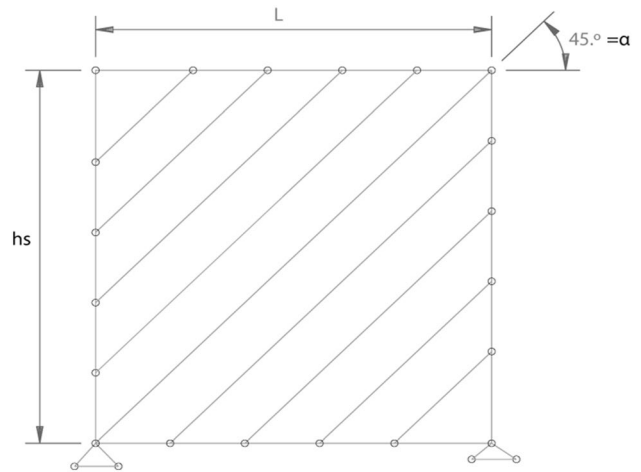


Fig. 4 The angle of the DCIP with the frame (based on Strip model)

plate and the boundary elements were modeled by utilizing a four-node quadrilateral shell element that is an element with reduced integration and large-strain formulation. Moreover, based on the findings regarding to the sensitivity analysis of the mesh, the size of 40 × 40 mm was considered for the boundary element as well as the infill plate. The solid element was used to mesh the Hysol adhesive plate that the mentioned solid element is an 8-node linear brick with reduced integration. According to the sensitivity analysis, the global mesh size of 10 × 10 mm was considered for the adhesive plate.

The connections of the boundary elements were fully moment resisting. Tie constrain was considered for the connection between the infill plate and the boundary elements. Concerning SBR-SPSW, each surface of the adhesive plate was tied with DCIPs.

The three transitional degrees of freedoms—U1, U2, and U3—were considered zero for the bottom ends of VBEs as illustrated in Fig. 1. And the degree of freedom—U3—was considered zero for the z-axis displacements of the top ends of VBEs and HBE to prevent the out-of-plane displacement of the SPSW. Displacement loading control method was applied for monotonic and cycle loading in both the nonlinear pushover and cyclic analyses at the axis top HBE. The stress–strain relationship of the steel material was considered

by the elastic–plastic model along with the kinematic hardening rule. A572 grade 50 steel and A36 steel constitute the components of the boundary elements and infill plates, respectively (ASTM A36, 2017). Table 2 represents a brief of the mechanical properties. Elastic modulus of 30 MPa and Poisson's ratio of 0.38 are the features representing the Hysol adhesive bonding material (Da Silva & Adams, 2005).

In the ATC24, for considering the nature of the loading cycle, as well as reduction of the errors and measurement of the force, the first five cycles (each for three times), and the last two cycles (each twice) were repeated, are shown in Fig. 5 ATC24 (1992). According to the FEMA-p750 (2009), the maximum drift ratio is 2.5%. Here is an important point to be noted in the ATC24 that increasing displacement is expressed as a percentage of the Δy . On the other hand, drift ratio is considered to be 2.5%. Therefore, to better compare cyclic and uniform loading with each other, the maximum displacement of the last cyclic loading is considered to be a drift ratio of 2.5%, and since the last cycle is considered to be a $500\% \Delta y$, i.e. Δy has been obtained and other cycles are calculated on the basis of that.

Validation on the finite element model of the SBR-SPSW

SPSW made by 2DCIPs is a new SPSW that has not been studied experimentally until now. To validate, the model studied by Wang et al. (2017) was examined by the finite element analysis. Furthermore, to verification of the SPSW with CIP, the finite element model was made and analyzed according to the experimental study of conducted by Emami et al. (2013).

To validate the model with 8 mm thickness, infill plates were selected according to the study of Wang et al. (2017). They investigated the seismic behavior of the SBR-SPSW made by two incline-slotted infill plates (2ISIPs). They examined four different infill plates with different thicknesses. Other geometric dimensions of the mentioned study are shown in Table 1. They also used Q235 steel for the infill plate and Q345 steel for the boundary elements as Table 2, and the rubber adhesive with an elastic modulus of 7.8 MPa and a Poisson ratio of 0.4. The first buckling mode shown in Fig. 6 was considered with amplitude of $\sigma_o = \sqrt{L \times h}/1000$

Table 2 Mechanical properties of materials

Steel type	F_y Mpa	F_U	ρ	E_o Gpa
Q235	235	410	0.3	210
Q345	345	460	0.3	210
A36	248	400	0.3	200
A572grade50	345	448	0.3	200

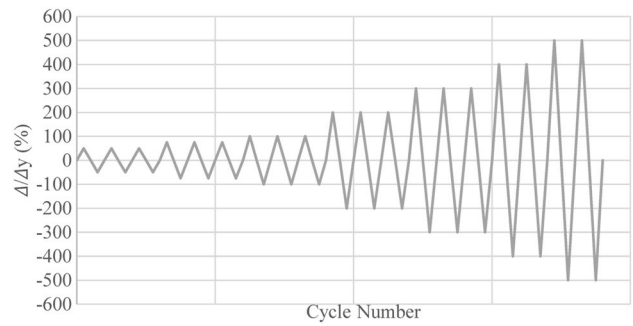


Fig. 5 Quasi-static displacement control loading sequence

as the initial geometric imperfection (Behbahanifard et al., 2003). The boundary conditions of the present study were the same that is mentioned in the finite element model by Wang et al. with the difference that the load was applied at the right end of top HBE. In Fig. 7, the monotonic force–displacement curve and the hysteretic curve obtained from the present analyses and the study of Wang et al. are shown in both elastic and elastic–plastic regions. According to the figure, the curves of both analyses are approximately coincident and so behaviors are almost similar.

To validate the SPSW with CIP, one finite element model was analyzed according to the specimen No.3 tested by Emami et al. (2013) under cyclic loading. The material properties of the infill plate and the boundary frame members were employed from the study conducted by Emami et al. (2013). Test setup and Dimension of the Specimen No.3 are shown in Fig. 8a, b. Finite element model as well as force-displacement diagram of the present study are indicated in Fig. 8c, d. As shown in Fig. 8d, the hysteretic curve of the finite element analysis and the tested specimen are approximately coincident in both elastic and elastic–plastic regions.

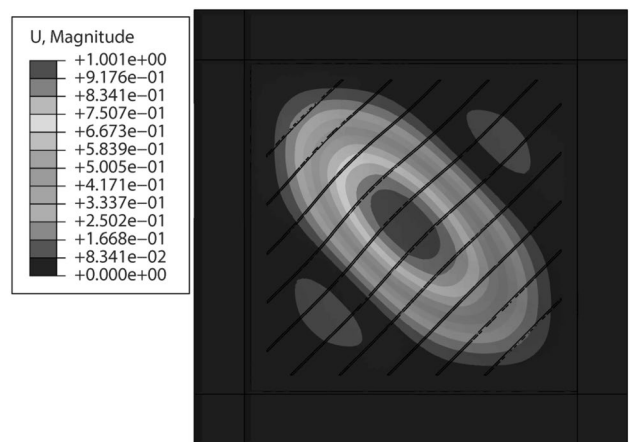


Fig. 6 Buckling mode of SBR-SPSW with 2ISIPs by Wang et al.

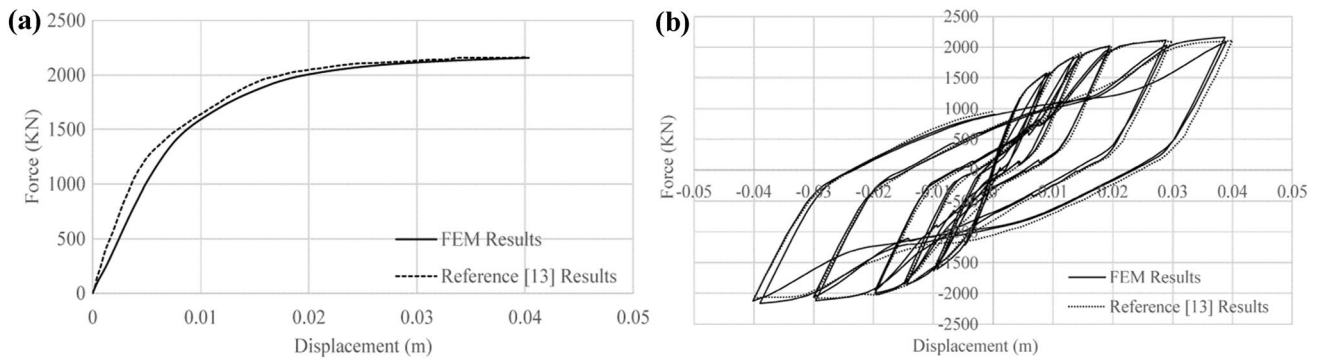


Fig. 7 Comparison between force–displacement curve by Wang et al. and FEM **a** monotonic; **b** cyclic

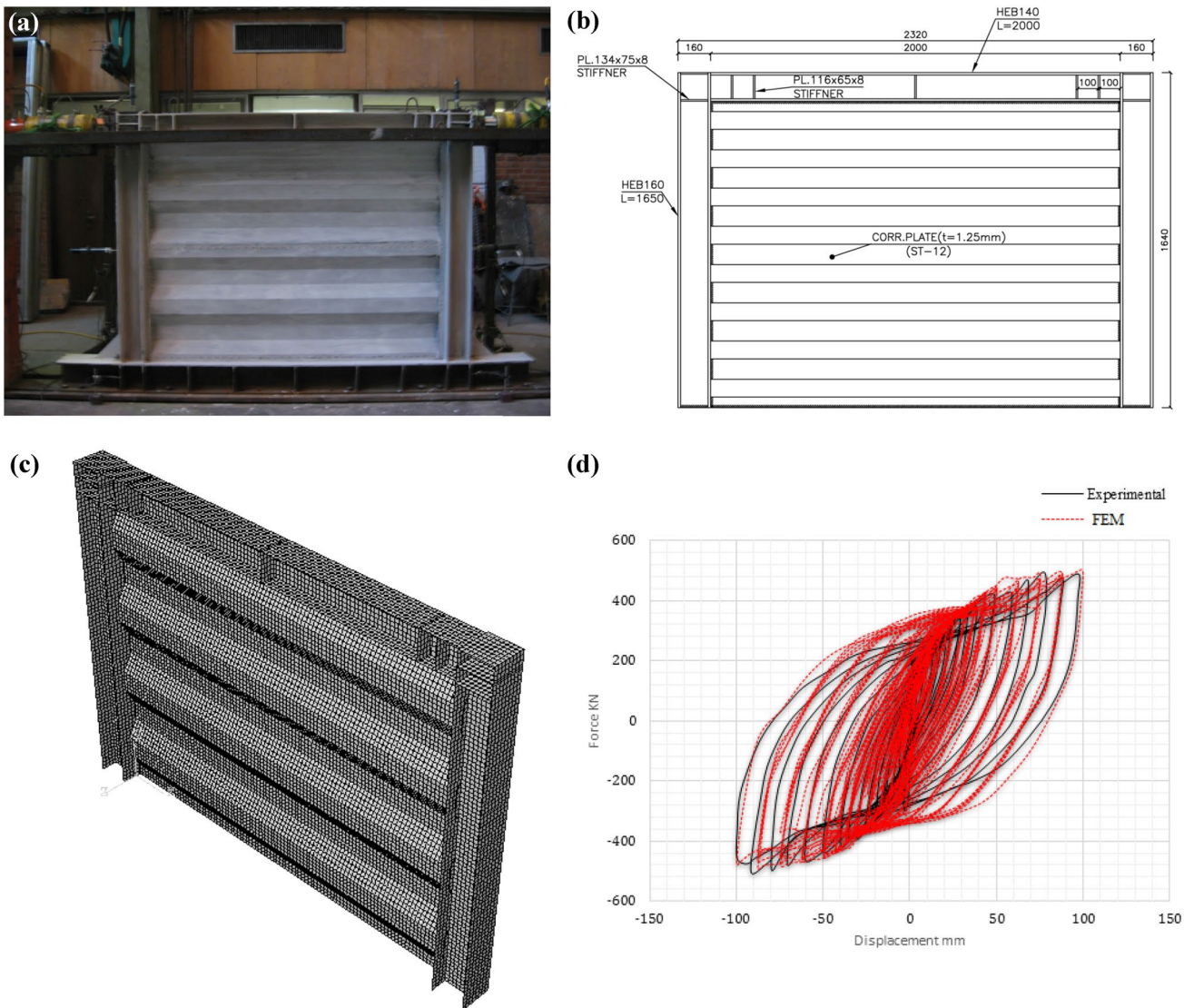


Fig. 8 FEM analysis of specimen No.3 (Emami et al., 2013) **a** Setup of specimen No.3 (Emami et al., 2013) **b** Dimension of model No.3 (Emami et al., 2013), **c** FEM model **d** Force–displacement diagram of test and analysis

The negligible difference is acceptable due to the idealistic modeling of material behavior and geometry as well.

The advantages of the SBR–SPSW made by 2DCIPs

To illustrate the advantages of this SBR-SPSW made by 2DCIPs, the shear strength, the formation of yield in the infill plates, beam and columns, response modification factor, the force applied to the column from the infill plates, buckling of the infill plates and energy dissipation have been investigated and compared with the SIP and CIP. It should be noted that the main samples with a t_w of 8 mm are investigated.

Improving shear strength

In all types of SPSWs, such as infill plates with slits, infill plates with opening, the use of LYP steel in the infill plates comparing to the SIP reduced the shear strength under monotonic loading and pushover analysis, but in the SBR-SPSW made by 2DCIPs, due to the use of two infill plates that provide lateral support for each other and resulting in limited buckling on the infill plate in comparison with the SIP, the shear strength increase of the infill plate was observed with overall thicknesses greater than 8 mm which is shown in Fig. 9.

Formation of the first yield on the infill plates, beam, and column, respectively

In the force–displacement curve under nonlinear pushover analyses (Fig. 9), it can be observed that due to the use of two 4 mm infill plates instead of one 8 mm infill plate and lateral support created by infill plates for each other, the first yielding has occurred at a LYP on the SBR-SPSW made by 2DCIPs. This behavior of the SBR-SPSW made by 2DCIPs is similar to the applying the LYP steel in the

SIP. Considering that the use of LYP infill plates is not economical and is caused reducing the ultimate shear strength compared to a SIP, the SBR-SPSW made by 2DCIPs can be used to reach the LYP in the infill plate without reducing the ultimate shear strength.

As shown in Fig. 9, yielding the infill plate in each of the three infill plates has always occurred before the boundary elements. But it is worth noting that the first yielding of the 2DCIPs occurred in a shear force about half of the shear force of the SIP. As mentioned due to considering the finite element model as one story the moment of inertia of the beam and the column was equal. With checking the first yield in the beam and column, it can be observed that the formation of the first yield of the beam was occurred in the model of the SBR-SPSW made by 2DCIPs and SPSW with SIP before the formation of the first yield in the column. There is little difference in the formation of the first yield in the beam and column due to the equality of the moment of inertia of the beam and the column which is expected to difference is more in the formation of the first yield in the beam rather than column in modeling of more stories. In the CIP, the first yield of the column was occurred before the first yield of the beam, which is due to the disadvantages of the CIP compared to the other infill plates in the mentioned thickness of the infill plate (8 mm).

It is noteworthy that due to the rigid column–foundation connection, it is necessary to design stiffeners in the connection area; therefore, in the investigation of the formation of the first yield in the column, the formation of the yield in the column–foundation connection was ignored.

Avoidance of shear strength drop in CIP

A study was conducted on the SPSW with a trapezoidal CIP (The direction of the waves was diagonal or, in other words, with a 45° angle) by Berman and Brno (2005). The hysteretic curves obtained from their study were asymmetric. Further, the studies were conducted on the SPSW with vertical and horizontal trapezoidal CIP by Emami et al. (2013). Although, an asymmetric hysteretic curve was not observed in the SPSW with CIP (vertical or horizontal wave) a shear strength drop was encountered in comparing with the SPSW with SIP. According to the results of the present study, in the SPSW made by 2DCIPs, due to the use of the DCIP, the shear strength was no longer accompanied by a strength drop. On the other hand, due to the use of 2DCIPs reversing each other and providing lateral support for each other, the hysteretic curve was not asymmetric, as shown in Fig. 10. In general, according to the results of this study, it can be said that the SPSW made by 2DCIPs has the advantages of both SPSW with vertical, horizontal and diagonal trapezoidal CIP for the infill plates with 8 mm thickness.

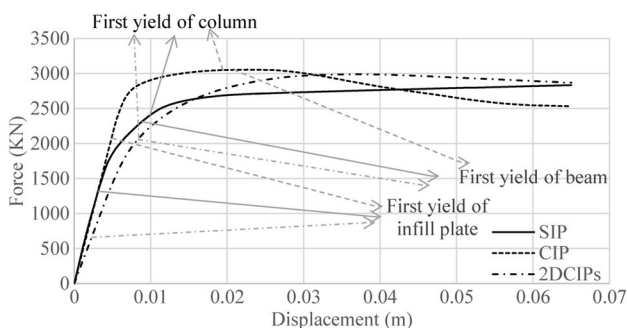


Fig. 9 Shear Strength of specimens under monotonic loading

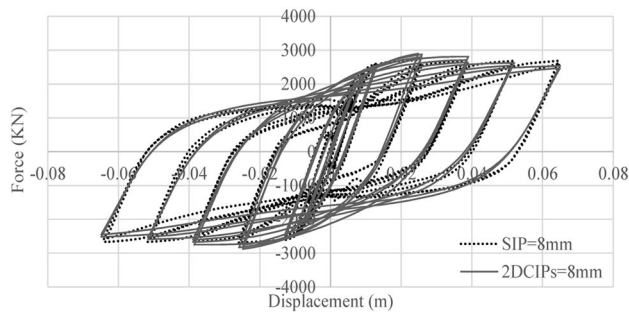


Fig. 10 Comparison of the hysteretic curve of the SPSW made by 2DCIPs and SIP

Increased energy dissipation

The energy dissipated in the SPSW depends on the three main components of the ultimate shear strength and the spindly hysteretic curve. As mentioned above, in the SPSW made by 2DCIPs, the ultimate shear strength and spindly hysteretic curve was increased compared with the SPSW with SIP as shown in Fig. 10. On the other hand, as shown in Fig. 10, the SPSW made by 2DCIPs has a spindly hysteretic curve in comparison to the SPSW with SIP. To compare the energy dissipation of the SPSW made by 2DCIPs and the SPSW with SIP, the inside areas of the hysteretic curves were compared with each other under a cyclic load. About 23% increase in energy dissipation was observed in the SPSW made by 2DCIPs compared to an SPSW with SIP.

In Fig. 11, the hysteretic curve of the SPSW made by 2DCIPs is comparable to the SPSW with CIP. In both cases, the effect of obesity or spindly curve is almost identical, but the SPSW with CIP has been faced with a drop in shear strength compared to the SPSW made by 2DCIPs. To compare the energy dissipation of the SPSW made by 2DCIPs and the SPSW with CIP, the inside areas of the hysteretic curves were compared with each other under a cyclic load. About 1% increase in energy dissipation was observed in the SPSW made by 2DCIPs compared to the SPSW with CIP

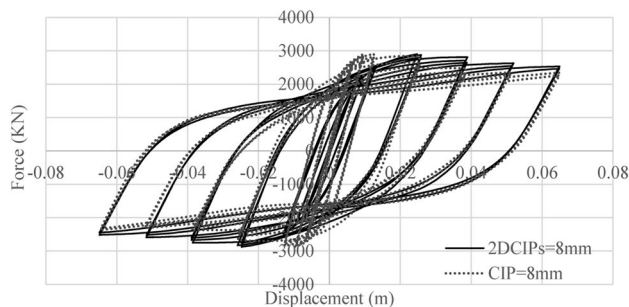


Fig. 11 Comparison of the hysteretic curve of the SPSW made by 2DCIPs and CIP

that can be said both samples almost have the same energy dissipation under this cyclic load.

In Fig. 12, the energy dissipation of each cycle is compared with the hysteretic curve in the SPSW made by 2DCIPs, the SPSW with SIP and CIP. The SPSW with SIP in all cycles has less energy dissipation than SPSW made by 2DCIPs and the SPSW with CIP. The SPSW with CIP in cycles with a displacement of less than 3 cm dissipates more energy than the SPSW made by 2DCIPs but in cycles with a displacement larger than 3 cm, the SPSW with CIP is facing with a shear strength drop and therefore totally the SPSW made by 2DCIPs has more energy dissipation than the SPSW with CIP.

Limitation of buckling on the SPSW made by 2DCIPs

With the formation of the diagonal tension field action, the greatest buckling always occurred on the two diagonals of the infill plates. Therefore, to compare the buckling of different types of the infill plates, the out of-plane displacement of both diagonals of the infill plate is discussed in this section. To check the different types of the infill plates in the same conditions, the out of-plane displacement of both diagonals was compared for the infill plates SBR-2DCIPs, SIP, and CIP under a lateral displacement of 6.5 cm, or a drift ratio of 2.5%. In Fig. 13, two paths are introduced on the diagonal of the infill plate and the out of-plane displacement of these two diagonal paths is compared with the same conditions in SBR-2DCIPs, CIP and SIP.

In Fig. 14(a), out of-plane displacement is visible on path 1 in the infill plates. SBR-2DCIPs has an out of-plane displacement maximum of about 10 cm in the middle of the infill plate on the diagonal, although the amount of out of-plane displacement was increased compared to SIP but is limited to a width of 0.5 to 1.2 m and it has less out of-plane displacement within 0 to 0.5 m and 1.2 to 2 m. Compared to CIP, the amount of out of-plane displacement is limited. In addition, SBR-2DCIPs have been relatively under tension or compression and

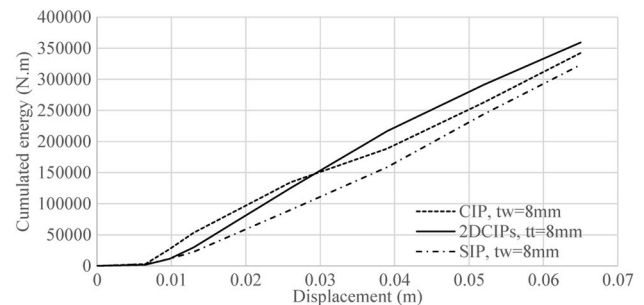


Fig. 12 Cumulated dissipated energy of the SPSWs with 2DCIPs, SIP and CIP

Fig. 13 Two diagonal paths are intended to determine out-of-plane displacement **a** path 2; **b** path 1

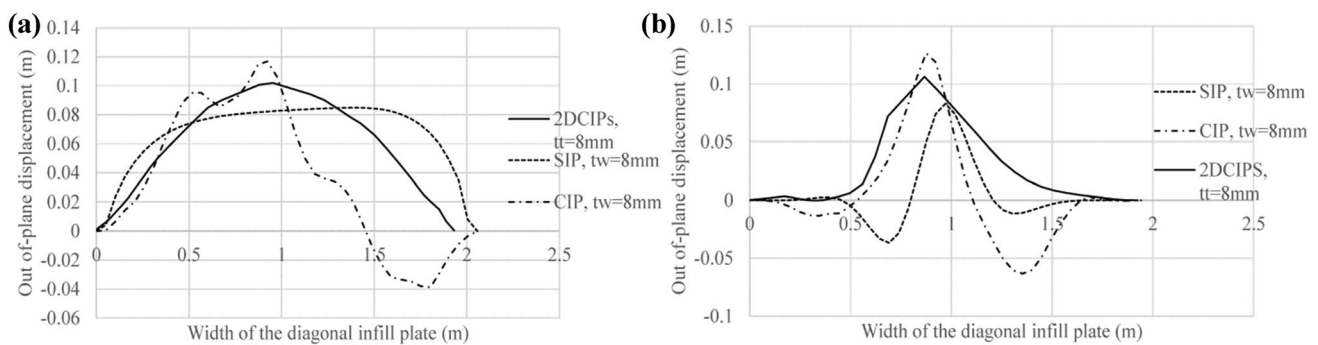
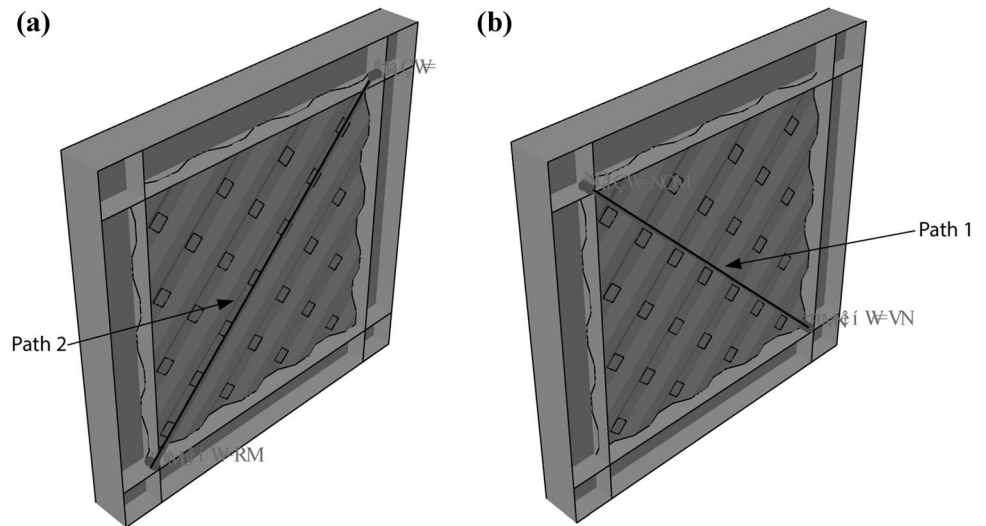


Fig. 14 Out-of-plane displacement of 2DCIPs, SIP and CIP **a** on path 1; **b** on path 2

out-of-plane displacements have not been observed in the negative direction.

In Fig. 14(b), the diagonal out-of-plane displacement curve is visible on path 2 in the infill plates. SBR-2DCIPs, like the previous one, have a greater out-of-plane displacement in comparison to SIP, but for SIP, out-of-plane displacement is also observed in the negative direction, which indicates the state of being under tension and compression of SIP. The other side on SBR-2DCIPs has not been seen out-of-plane displacement in the negative direction, which is displayed under the tension or compression of SBR-2DCIPs. Compared to CIP, the amount of out-of-plane displacement on the diagonal is reduced, and for CIP the same of SIP, there is also an out-of-plane displacement in the negative direction, which indicates that the plate is always under the tension and compression of CIP. The buckling is limited on SBR-2DCIPs, which leads to no crack formation occurring under repeated shear buckling.

Reduction of force on the column from the infill plates

SBR-2DCIPs consists of two DCIPs, each of which is individually applied the force into the column. First, the force applied to the column was examined from each of the DCIPs; then, the total force of both DCIPs was considered as the force applied to the column from SBR-2DCIPs and is compared with the force applied to the column from SIP and CIP. It should be noted that all specimens were fitted with the infill plate thickness of 8 mm and moved to lateral displacement of 6.5 cm. Under a drift ratio of 2.5% and in a completely identical situation, different infill plates were compared.

In Fig. 15, the horizontal and vertical forces applied to the column are visible. The forces applied on the total height of the column from both DCIPs of SBR-2DCIPs. One of the DCIPs is relatively under tension and the other under compression. The sum of the force from both DCIPs was

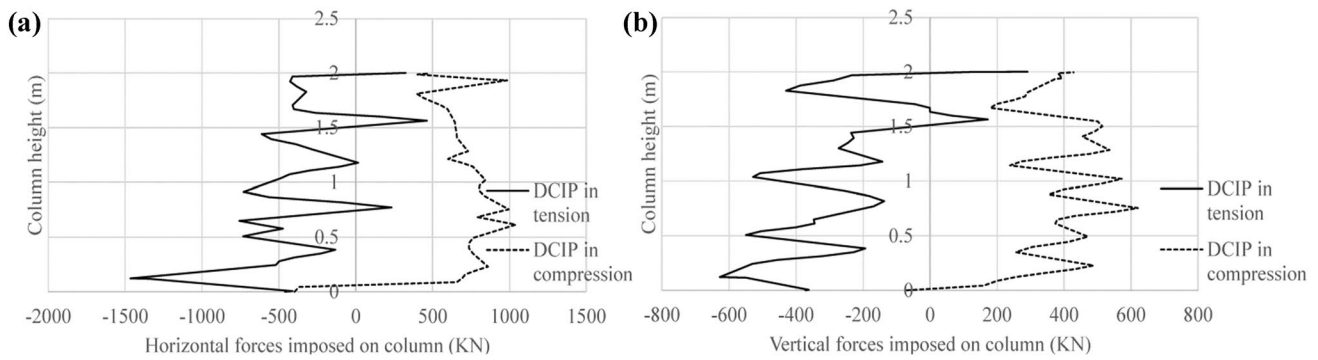


Fig. 15 The force applied into the column from both of DCIP **a** horizontal force; **b** vertical force

considered as the force from SBR-2DCIPs and when one infill plate is under tension and the other under compression, the neutral force is approximately applied to the column.

In Fig. 16, the vertical and horizontal forces applied to the column are plotted on SBR-2DCIPs, SIP, and CIP based on the height of the column. The horizontal and vertical forces of SBR-2DCIPs applied to the column were decreased in the most places compared to SIP and CIP. Thus, the use of two DCIPs, which are relatively under tension and compression, resulted in a decrease in the force applied to the column from the SBR-2DCIPs compared to the SIP and CIP.

Improvement of the response modification factor(R)

In Table 3, the response modification factor and the ductility factor obtained by the relations provided by Uang have been presented (1991). By comparing the response modification factor of the Uang method in the SBR-SPSW made by 2DCIPs, the SPSW with SIP and CIP, it can be observed that the SBR-SPSW made by 2DCIPs has a smaller response modification factor than the SPSW with SIP in thicknesses of 4 to 8 mm, but in thicknesses of 2, 3 and 10 mm, the response modification factor of the SBR-SPSW made by 2DCIPs increases in comparison with the SPSW with SIP.

Further, the SBR-SPSW made by 2DCIPs has a higher response modification factor than SPSW with CIP in all thicknesses. In this section, the response modification factor with related parameters as well as the ductility factor of the frame without the infill plate is also calculated and compared to the SPSWs with infill plates. The observed response modification factor of the SPSW has always significantly increased rather than that of the frame. In the SPSW made by 2DCIPs and the SPSW with CIP, when the infill plates thickness was decreased from 10 to 2 mm, the response modification factor increased, but in the SPSW with SIP, when the infill plate thickness was decreased from 8 to 4 mm, the response modification factor increased first and then, in the thicknesses less than 4 mm and more than 8 mm, the response modification factor decreased.

In general, it can be said that the SPSW made by 2DCIPs in thickness of 2, 3 and 10 mm in comparison with the SPSW with SIP has a higher response modification factor. Although in the thicknesses of 4 and 8 mm, it has a lower response modification factor than the SPSW with SIP, it always has a higher response modification factor than the SPSW with CIP. By decreasing the thickness of the infill plates of the SPSWs, the elastic stiffness always decreased, but in the SPSW made by 2DCIPs, elastic stiffness decrease

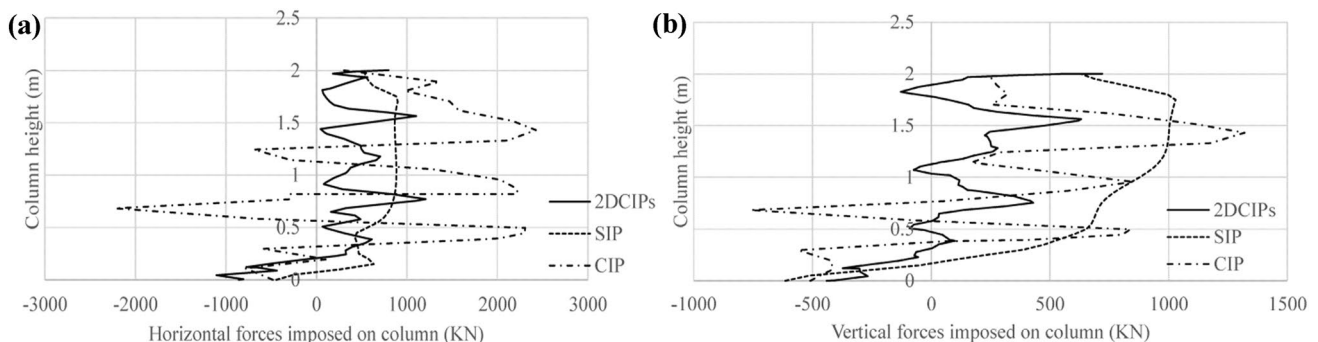


Fig. 16 The force applied into the column from 2DCIPs, SIP and CIP **a** horizontal force; **b** vertical force

Table 3 The response modification factor and the corresponding coefficients

	SPSW with Infill plates	t_w t_t (mm)	Ω_o	R_μ	R	μ_s	V_s (KN)	Δ_s (mm)	K_e (KN/mm)
1	SPSW made by 2DCIPs	10	1.59	3.38	5.4	6.2	2047.3	6.56	311.85
2	SPSW with SIP	10	1.2	4.24	5.11	9.32	2491	5.78	430.6
3	SPSW with CIP	10	1.16	3.63	4.24	7.77	3235.2	7.15	452.47
4	SPSW made by 2DCIPs	8	1.65	3.41	5.64	6.29	1722.18	6.24	275.99
5	SPSW with SIP	8	1.44	4.36	6.29	9.6	1793.9	4.68	383.3
6	SPSW with CIP	8	1.2	3.81	4.63	8.47	2571	6.305	407.772
7	SPSW made by 2DCIPs	4	1.77	3.72	6.6	7.14	974.36	5.13	189.78
8	SPSW with SIP	4	2.2	4.03	8.97	8.02	820.49	3.64	225.41
9	SPSW with CIP	4	1.3	4.33	5.63	9.85	1361.71	5.07	268.582
10	SPSW made by 2DCIPs	3	1.83	3.85	7.05	7.38	781.19	4.81	162.41
11	SPSW with SIP	3	1.82	3.73	6.81	6.9	882.51	5.13	171.86
12	SPSW with CIP	3	1.35	4.36	5.92	9.69	1079.32	4.94	218.486
13	SPSW made by 2DCIPs	2	2.18	3.88	8.47	7.23	536.29	4.11	130.26
14	SPSW with SIP	2	1.93	3.61	6.99	6.45	704.66	5.2	135.512
15	SPSW with CIP	2	1.43	4.75	6.82	10.23	751.326	4.428	169.676
16	Frame without infill plate		1.23	2.3	2.85	3.05	795.05	17.1	46.27

was less observed, with a thickness of 8 mm, elastic Stiffness was significantly reduced compared to the SPSW with SIP and CIP and in a thickness of 2 mm, the elastic stiffness was almost equal in each of the three specimens and no significant difference was observed, which increased the response modification factor of the SPSW made by 2DCIPs compared to the SPSW with SIP.

Parametric study on the SPSW made by two 2DCIPs

In this section, the influence of geometric parameters of the infill plate is investigated such as infill plate thickness, the angle of the sub-plates of the CIP, the angle of the DCIP with the frame, the wavelength of corrugation and the adhesive thickness. For more accurate examination and analysis of each of the parameters separately, all geometric parameters except the corresponding parameter are considered according to the mentioned geometric specifications.

The effect of infill plate thickness

To compare the infill plate thickness, ten SIPs and CIPs were designed with thicknesses (t_w) of 2, 3, 4, 8 and 10 mm and five 2DCIPs with total thicknesses (t_t) of 2, 3, 4, 8 and 10 mm. All samples were analyzed under a nonlinear pushover analysis. The shear force–displacement diagram is shown in Fig. 17 and Fig. 18. The SPSW made by two 2DCIPs with a total thickness (t_t) equal or greater than 8 mm in comparison to the SIP with the same thickness,

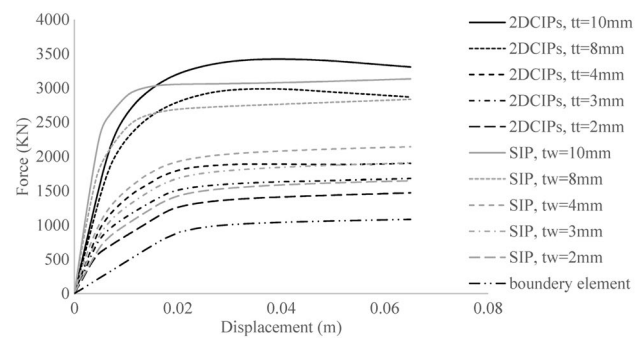


Fig. 17 Comparison of the different thicknesses of the SBR-SPSW made by 2DCIPs, SPSW with SIP

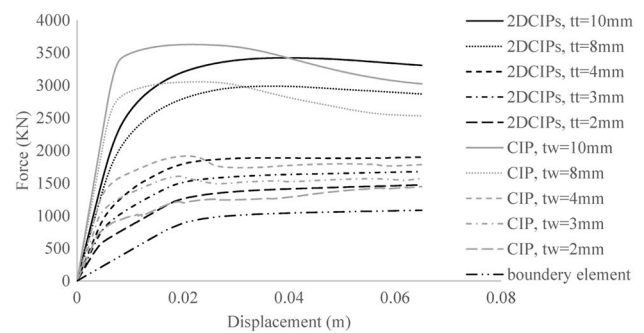


Fig. 18 Comparison of the different thicknesses of the SBR-SPSW made by 2DCIPs, SPSW with CIP

although the elastic stiffness decreased the ultimate strength increased, as shown in Fig. 17. Therefore, this comparison is well illustrated one of the advantages of the SPSW made by 2DCIPs that in infill plates with overall total thicknesses equal or greater than 8 mm has a greater ultimate strength compared to the SPSW with SIP of the same thickness. In this study, the shear force–displacement curve of the frame without the infill plate is also included to examine the shear strength of the infill plates. The ultimate shear strength of the frame without the infill plate is observed at around 1083 KN which is very lower than that of the SPSW.

Table 4 shows the ultimate shear strength of the infill plates, regardless of the ultimate shear strength of the surrounding frame. SIP in thicknesses less than 4 mm, compared to 2DCIPs and CIP, has a higher ultimate shear strength but has a lower ultimate shear strength in the thicknesses more than 8 mm. Here, one of the weaknesses of SIP is clearly visible that the shear strength was not increased with increasing thickness, appropriately. Therefore, it is always advisable to use thin SIP and 2DCIPs have somewhat improved the weakness of the SIP.

In the SPSW with horizontal CIP in different thicknesses, a drop in the shear strength was observed, as shown in Fig. 18. The remarkable point in this study is that with increasing the thickness of the CIP from 2 to 10 mm, the shear strength drop has been transmitted approximately from the displacement of 1.2 cm to 3 cm. Although in all specimens, the CIP has a higher ultimate strength compared to the SPSW made by 2DCIPs, with a total thickness greater than 8 mm, a significant shear strength drop is observed.

Table 4 The ultimate shear strength of the infill plates, regardless of the ultimate shear strength of the frame

	Infill plates	Thicknesses (mm)	Ultimate shear strength (KN)
1	2DCIPs	10	2338
2	2DCIPs	8	1904
3	2DCIPs	4	815
4	2DCIPs	3	594
5	2DCIPs	2	389
6	SIP	10	2048
7	SIP	8	1783
8	SIP	4	1057
9	SIP	3	815
10	SIP	2	565
11	CIP	10	2539
12	CIP	8	1971
13	CIP	4	826
14	CIP	3	519
15	CIP	2	362

The effect of the angle of the sub-plates of the CIP (θ)

The angles of 15, 30, 45, 60 and 90 degrees were considered to examine the effect of the angle of the sub-plates of the DCIP. By comparing different angles with each other, as shown in Fig. 19, it can be concluded that with increasing the angle of the sub-plates of the DCIP, the ultimate shear strength always increases. Here is an important point: with the increase in the angle of the sub-plates of the DCIP, the weight of DCIP always increases. In Table 5, weight gain at different angles is shown in comparison with SIP in the same thickness. For example, the angle of 90° has the highest ultimate shear strength but its weight becomes twice. The angle of 15° has the least weight gain (about 101.7%) but instead a significant reduction in shear strength is observed in comparison with other angles. In 30°, 45°, and 60°, there is not much difference in the shear strength, but in respect of weight, the angle of 30° has the lowest value (about 107%). By comparing the weight gain and the ultimate strength at different angles, it can be concluded that the angle of 30° is the most optimal angle for the angle of the sub-plates of the DCIP.

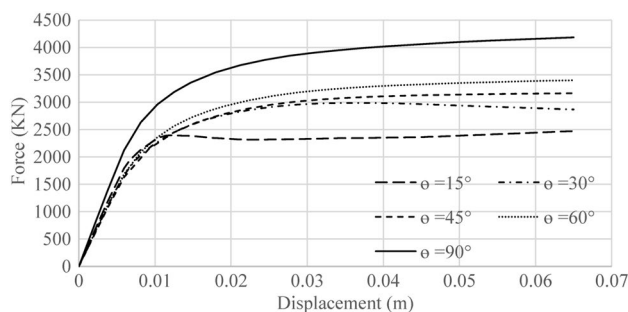


Fig. 19 The effect of the angle of the sub-plates of the CIP on the shear strength of SBR-SPSW made by 2DCIPs

Table 5 Percentage of overweight is based on the angle of the sub-plates of the CIP compared to the SIP

	The angle of the sub-plates of the CIP	W_{DCIP}/W_{SIP} (%)	Ultimate strength(KN)
1	15	101.7	2471
2	30	107.17	2866
3	45	117	3164
4	60	133	3401
5	90	200	4185

Comparison of the effect of weight versus the increase in angle of the sub-plates of the CIP

In the previous section, the ultimate shear strength was improved by increasing the angle of the sub-plates of the CIP (θ) but with increasing the angle, the weight of the infill plate also increased. Therefore, for a more accurate examination, a SPSW made by 2DCIPs with the angle of the sub-plates 90-degree and a total thickness of 4 mm was modeled. According to the Table 5, when the angle of the sub-plates of the DCIP is considered to be 90°, the weight of the infill plate will be double. Thus, the overall thickness of the 2DCIPs is considered 4 mm which it can be compared to the SPSW made by 2DCIPs with the angle of the sub-plates of the CIP 30° but total thickness of 8 mm and the SPSW made by SIP and thickness of 8 mm, which is visible in Fig. 20. By increasing the angle of the sub-plates of the CIP, no increase was observed in ultimate shear strength in almost equal weight conditions. Therefore, as mentioned in the previous section, when the angle of the sub-plates of the CIP is 30 degrees the optimum angle of the sub-plates of the CIP is obtained due to the weight of the 2DCIPs and also the ultimate shear strength.

The effect of the angle of the DCIP with the frame (a)

To examine the effect of the angle of the DCIP with the frame, four angles of 30, 42, 45, and 60 degrees were compared. According to Eq. 6 and geometric characteristics, the angle of the DCIP with the frame (α) or, in other words, the angle of formation of the diagonal tension field is 42 degrees. As shown in Fig. 21, the models with angles 30 and 60 degrees show the same behavior with a shear strength drop but the models with angles 42 and 45 have approximately the same behavior without shear strength drop. According to Eq. 6, the angle of the formation of the

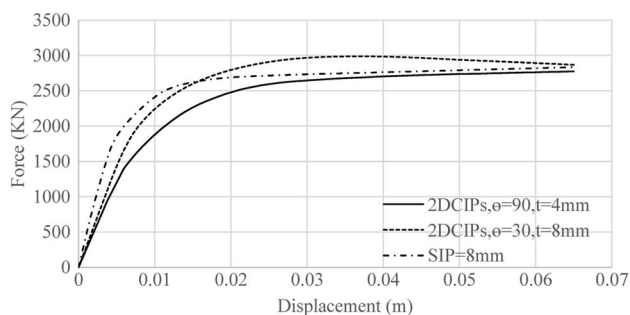


Fig. 20 Comparison of the shear strength of the SPSW with SIP and SBR-SPSW made by 2DCIPs with two angles of the sub-plates of the CIP 30 and 90 degrees

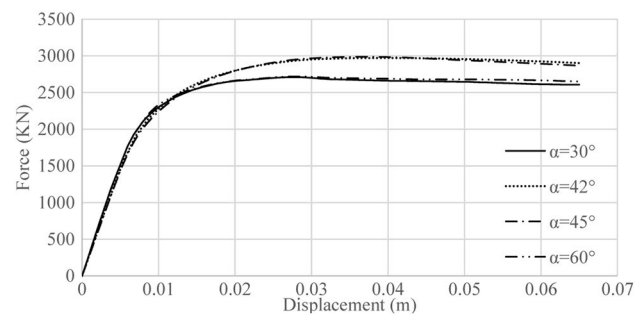


Fig. 21 The effect of the angle of the DCIP with the frame

diagonal tension field varies with the thickness of the infill plates. Further, the ultimate shear strength of the models with the angles of 45 degrees and 42 degrees doesn't have difference. Therefore, the angle of 45 degrees is considered as an optimal angle, so that in the examination of different thicknesses, only the thickness of the infill plates has been changed and the angle of the DCIP with the frame fixed of 45 degrees is considered.

The effect of the sub-plate width (Lw)

To investigate the effect of the sub-plate width (L_w) on the SPSW made by 2DCIPs, five samples were studied. The sub-plate width of 5, 8, 10, 12, and 15 cm was selected for the study. Shear force–displacement curves obtained from nonlinear pushover analyses were compared with each other, as shown in Fig. 22. By comparing the curves, it can be seen that the sample with the sub-plate width of the 10 cm has higher ultimate shear strength than the other specimens, except of the sample with the sub-plate width of 12 cm, but the 12 cm sub-plate width sample has a smaller initial stiffness. Considering that by increasing or decreasing the sub-plate width from 10 cm to 15 or 5 cm, the decrease of shear strength is observed. Thus, the sub-plate width is 10 cm as optimal.

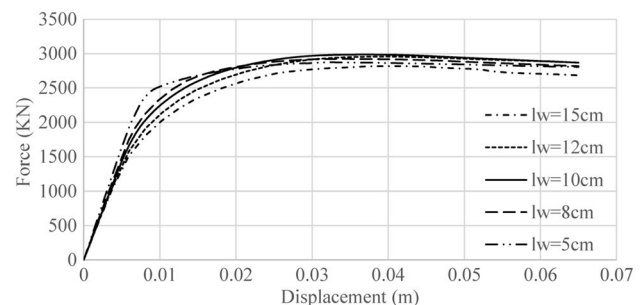


Fig. 22 The effect of sub-plate width on the shear strength of SBR-SPSW made by 2DCIPs

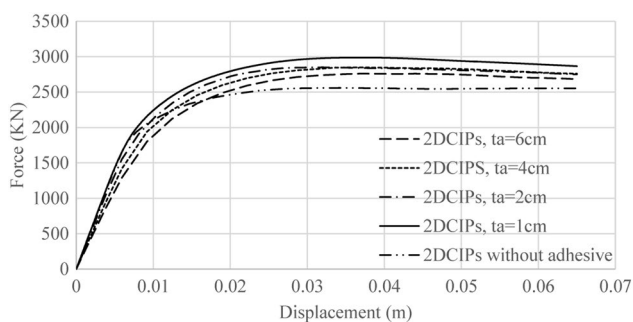


Fig. 23 The effect of adhesive thickness on the shear strength of SBR-SPSW made by 2DCIPs

The effect of adhesive thickness

For investigating the effect of eccentricity of the infill plates and the effect of adhesive thickness (t_a) on the energy dissipation, four adhesive thicknesses of 1, 2, 4 and 6 cm were modeled. As shown in Fig. 23, the ultimate shear strength decreases with increasing the adhesive thickness. The eccentricity of the infill plates, which is accompanied by increase in the adhesive thickness, leads to a reduction in the ultimate shear strength and the energy dissipation. It is noteworthy that, in the thicknesses less than 1 cm, the adhesive does not behave well in out-of-plane displacement, resulting in a lack of convergence in the solution. For this reason, the adhesive thickness is 1 cm as the optimum adhesive thickness. Furthermore, Compared to the SPSW made by 2DCIPs, with an adhesive thickness of 1 cm and without adhesive, clearly the effect of adhesive is visible. With using adhesive, the infill plates provide for each other the lateral support and limit the buckling of the infill plates. The limitation of the buckling of the infill plates has led to a significant increase in shear strength in the SPSW made by 2DCIPs. Moreover, according to the shear force–displacement curve of the without adhesive specimen, it is clear that using DCIP has postponed the shear strength drop in the SPSW made by 2DCIPs to the displacement of 6.5 cm.

Conclusion

In this study, the seismic behavior of the new SPSW made by 2DCIPs was investigated. The SPSW made by 2DCIPs consists of two DCIPs being tied to each other with Hysol adhesive. The direction of two DCIPs is reverse. Firstly, the effect of the parameters of this new infill plate, such as infill plate thickness, the angle of the DCIP with the frame, sub-plate width, the angle of the sub-plates of the DCIP and adhesive thickness in this new SPSW were investigated and then the optimum infill plate was introduced.

Because of the use of DCIP, the SPSW made by 2DCIPs does not encountered shear strength drop unlike the SPSW with CIP. By entering lateral force to the frame, one of the DCIPs is relatively under compression and the other DCIP under tension, which leads to a reduction in the force from the infill plate to the column compared to the SIP and CIP. The DCIP under tension provides the lateral support for the DCIP under compression, resulting in limited buckling of this new infill plate. The imitated buckling of the infill plate prevents the crack formation which occurs under repeated shear buckling and also results in an increase in the shear strength of the SPSW made by 2DCIPs with the infill plates in thicknesses greater than 8 mm in comparison to the SPSW with SIP. Using two infill plates of DCIP in the SPSW instead of one SIP in the SPSW, the yield formation of the SBR-2DCIPs occurs at the lower yield point whereas the yield of the beam and columns occurs with more delay.

Although the response modification factor of the SPSW made by 2DCIPs decreases slightly in some thicknesses compared to the SPSW with SIP, but it has a significant increase compared to the SPSW with CIP.

In the SPSW made by 2DCIPs, the hysteretic curve is stable and spindle-shape which resulting in an increase of 23% in energy dissipation compared to the SPSW with SIP and an increase of 1% in energy dissipation compared to the SPSW with CIP under ATC24 cyclic loading.

The SPSW with SIP and CIP have advantages and disadvantages. In general, it can be said that the SPSW made by 2DCIPs according to the results of this study has almost all the advantages of the SPSW with SIP and CIP. Even in some cases, it is shown a convenient behavior. The SPSW made by 2DCIPs with high-thickness infill plates is proposed for high-rise structures with large Base shear. In this study, this new SPSW was introduced investigated in some parameters. Further investigation is proposed such as the location of the infill plates in the frame, the effect of the height-width ratio of the bay, the number of the floors and also the number of the bays.

Funding The authors have not disclosed any funding.

Declarations

Conflict of interest On behalf of all authors, the corresponding author states that there is no conflict of interest.

References

- AISC 341–10. (2010). *Seismic Provisions for Structural Steel Buildings*. Chicago: American Institute of Steel Construction.
- Ali, M. M., Osman, S. A., Husam, O. A., & Al-Zand, A. W. (2018). Numerical study of the cyclic behavior of steel plate shear wall

- systems (SPSWs) with differently shaped openings. *Steel and Composite Structures*, 26(3), 361–373.
- Astaneh-Asl, A. (2001). “Seismic behavior and design of steel shear walls”, Paper Distributed and presented at the 2001 SEOANC Seminar, Structural Engineers Assoc. of Northern California, November 7, San Francisco.
- ASTM A36, (2017), Standard Specification for Carbon Structural Steel, A572. Standard Specification for High-Strength Low-Alloy Columbium-Vanadium Structural Steel.
- ATC-24 (1992), Guidelines for cyclic testing of components of steel structures, Stanford (California), Stanford University.
- Behbahani, M. R., Grondin, G. Y., & Elwi, A. E. (2003). “*Experimental and numerical investigation of steel plate shear walls* Structural Engineering Report No. 254. University of Alberta, Department of Civil and Environmental Engineering.
- Berman, J. W., & Bruneau, M. (2005). Experimental investigation of light-gauge steel plate shear walls. *Journal of Structural Engineering*, 131, 259–267. [https://doi.org/10.1061/\(ASCE\)0733-9445\(2005\)131:2\(259\)](https://doi.org/10.1061/(ASCE)0733-9445(2005)131:2(259))
- Bhowmick, A. K., Grondin, G. Y., & Driver, R. G. (2014). Nonlinear seismic analysis of perforated steel plate shear walls. *Journal of Constructional Steel Research*, 94, 103–113. <https://doi.org/10.1016/j.jcsr.2013.11.006>
- Caccese, V., Elgaaly, M., & Chen, R. (1993). Experimental study of thin steel-plate shear walls under cyclic load. *Journal of Structural Engineering*, 119, 573–587. [https://doi.org/10.1061/\(ASCE\)0733-9445\(1993\)119:2\(573\)](https://doi.org/10.1061/(ASCE)0733-9445(1993)119:2(573))
- Da Silva, L. F., & Adams, R. (2005). Measurement of the mechanical properties of structural adhesives in tension and shear over a wide range of temperatures. *Journal of Adhesion Science and Technology*, 19, 109–141. <https://doi.org/10.1163/1568561053148449>
- Dou, C., Pi, Y. L., & Gao, W. (2018). Shear resistance and post-buckling behavior of corrugated panels in steel plate shear walls. *Thin-Walled Structures*, 131, 816–826. <https://doi.org/10.1016/j.tws.2018.07.039>
- Dou, C., Cheng, X., Zhao, Y. Y., & Yang, N. (2021). Shear resistance and design of infill panels in corrugated-plate shear walls. *Journal of Structural Engineering*, 147(11), 04021179.
- Driver, R. G., Kulak, G. L., Elwi, A. E., & Kennedy, D. L. (1998). FE and simplified models of steel plate shear wall. *Journal of Structural Engineering*, 124, 121–130. [https://doi.org/10.1061/\(ASCE\)0733-9445\(1998\)124:2\(121\)](https://doi.org/10.1061/(ASCE)0733-9445(1998)124:2(121))
- Edalati, S. A., Yadollahi, Y., Pakar, I., & Bayat, M. (2015). On the effect of GFRP fibers on retrofitting steel shear walls with low yield stress. *Earthquakes and Structures*, 8(6), 1453–1561.
- Elgaaly, M. (1998). Thin steel plate shear walls behavior and analysis. *Thin-Walled Structures*, 32, 151–180. [https://doi.org/10.1016/S0263-8231\(98\)00031-7](https://doi.org/10.1016/S0263-8231(98)00031-7)
- Elgaaly, M., Caccese, V., & Du, C. (1993). Postbuckling behavior of steel plate shear walls under cyclic loads. *Journal of Structural Engineering*, 119, 588–605. [https://doi.org/10.1061/\(ASCE\)0733-9445\(1993\)119:2\(588\)](https://doi.org/10.1061/(ASCE)0733-9445(1993)119:2(588))
- Emami, F., & Mofid, M. (2014). On the hysteretic behavior of trapezoidally corrugated steel shear walls. *The Structural Design of Tall and Special Buildings*, 23(2), 94–104. <https://doi.org/10.1002/tal.1025>
- Emami, F., Mofid, M., & Vafai, A. (2013). Experimental study on cyclic behavior of trapezoidally corrugated steel shear walls. *Engineering Structures*, 48, 750–762. <https://doi.org/10.1016/j.engstruct.2012.11.028>
- Hitaka, T., & Matsui, C. (2003). Experimental study on steel shear wall with slits. *Journal of Structural Engineering*, 129, 586–595. [https://doi.org/10.1061/\(ASCE\)0733-9445\(2003\)129:5\(586\)](https://doi.org/10.1061/(ASCE)0733-9445(2003)129:5(586))
- Kalali, H., Hajsadeghi, M., Zirakian, T., & Alaei, F. A. (2015). Hysteretic performance of SPSWs with trapezoidally horizontal corrugated web-plates. *Steel and Composite Structures*, 19(2), 277–292.
- Kaveh, A., & Farhadmanesh, M. (2019). Optimal seismic design of steel plate shear walls using metaheuristic algorithms. *Periodica Polytechnica*, 63(1), 1–17.
- Nakashima, M., Iwai, S., Iwata, M., Takeuchi, T., Konomi, S., Akazawa, T., & Saburi, K. (1994). Energy dissipation behavior of shear panels made of low yield steel. *Earthquake Engineering & Structural Dynamics*, 23, 1299–1313. <https://doi.org/10.1002/eqe.4290231203>
- NEHRP recommended seismic provisions for new buildings and other structures (FEMA P-750) (2009), Federal Emergency Management Agency, Washington DC
- Qu, B., & Bruneau, M. (2011). Plastic moment of intermediate horizontal boundary elements of steel plate shear walls. *Engineering Journal-Chicago*, 48, 49.
- Roberts, T. M., & Sabouri-Ghomi, S. (1992). Hysteretic characteristics of unstiffened perforated steel plate shear panels. *Thin-Walled Structures*, 14, 139–215. [https://doi.org/10.1016/0263-8231\(92\)90047-Z](https://doi.org/10.1016/0263-8231(92)90047-Z)
- Shariati, M., Safaei Faegh, S., Mehrabi, P., Bahavarnia, S. M., Zandi, Y., Rezaee Masoom, D., Toghrol, A., Trung, N., & Salih, M. (2019). Numerical study on the structural performance of corrugated low yield point steel plate shear walls with circular openings. *Steel and Composite Structures*, 33(4), 569–581.
- Soltani, N., Abedi, K., Poursha, M., & Golabi, H. (2017). An investigation of seismic parameters of low yield strength steel plate shear walls. *Earthquakes and Structures*, 12(6), 713–723.
- Timler, P. A., & Kulak, G. L. (1983). “*Experimental study of steel plate shear walls*, Structural Engineering” Report No. 114. Department of Civil Engineering University of Alberta.
- Tong, J. Z., Guo, Y. L., & Pan, W. H. (2020). Ultimate shear resistance and post-ultimate behavior of double-corrugated-plate shear walls. *Journal of Constructional Steel Research*, 165, 1–14. <https://doi.org/10.1016/j.jcsr.2019.105895>
- Uang, C. M. (1991). Establishing R (or R w) and Cd factors for building seismic provisions. *Journal of Structural Engineering*, 117, 19–28. [https://doi.org/10.1061/\(ASCE\)0733-9445\(1991\)117:1\(19\)](https://doi.org/10.1061/(ASCE)0733-9445(1991)117:1(19))
- Wang, P., Xue, Z., & Xiao, S. (2017). Seismic behavior of Self-Buckling-Restrained Steel Plate Shear Wall made by two incline-slotted infill plates. *Journal of Constructional Steel Research*, 133, 47–64. <https://doi.org/10.1016/j.jcsr.2017.02.001>
- Zirakian, T., & Zhang, J. (2016). Study on seismic retrofit of structures using SPSW systems and LYP steel material. *Earthquakes and Structures*, 10(1), 1–23.